

# Electrochemical oxidation and polymerization of *N*-vinyl-thionaphthene-indole

G. CASALBORE-MICELI, G. BEGGIATO, S. S. EMMI, A. GERI

*Istituto di Fotochimica e Radiazioni d'Alta Energia del Consiglio Nazionale delle Ricerche, Via de' Castagnoli, 1, I-40126 Bologna, Italy*

S. DAOLIO

*Istituto di Polarografia ed Electrochimica Preparativa del Consiglio Nazionale delle Ricerche, Corso Stati Uniti, 4, I-35100 Padova, Italy*

Received 16 March 1988; revised 15 May 1988

The electrochemical behaviour of *N*-vinyl-thionaphthene-indole (VTNI) has been investigated and compared with that of other similar heterocyclic molecules. By electro-oxidation of VTNI in methylene chloride at +1.2 V an oxidized dimer or a black oxidized polymer have been obtained, depending on the monomer concentration. The polymeric material is a cross-linked structure with intermonomer bonds involving both aromatic rings and vinyl side groups.

## 1. Introduction

In the electrochemical synthesis of conducting or semi-conducting polymers, the study of the electrode process of the monomer and the optimization of the experimental parameters are two intimately linked problems. The chemical reactions of aromatics connected with the electron transfer are influenced not only by experimental factors, like solvent, temperature, current density, etc., but also by the aromatic ring substituents. As an example, by electrochemical oxidation of carbazoles, a dimer [1-4], a polymer with coupling sites localized on the aromatic rings [3, 4] or a cross-linked polymer, as in the particular case of *N*-vinyl-carbazole [5, 6], are obtained, depending on the experimental conditions. The widely studied electropolymerization of pyrrole is strongly dependent on and even hindered by  $\alpha$ -substituent groups [7, 8]. An analogous substituent-dependent behaviour was also observed for thiophenes [9], benzothiophenes [9] and thionaphthene-indoles [10-12]. When these last compounds, which show photoconducting properties [13], are electrochemically oxidized in methylene chloride on a platinum electrode, different products are obtained, depending on the nature of the side group linked to the N atom.

In the present work the electrochemical behaviour of *N*-vinyl-thionaphthene-indole (VTNI) is investigated and compared with both that of the unsubstituted monomer (TNI) [11, 14] and its *N*-allyl derivative (ATNI) [10, 15], and that of *N*-vinyl-carbazole (VCZ) [5, 6].

The results indicate the importance of the vinyl group linked to the N atom in the electropolymerization process, in accord with earlier results on VCZ.

## 2. Experimental details

Thionaphthene-indole (TNI) ([1 benzothieno [3,2-b] indole] (Fig. 1a) was obtained from *o*-thiolbenzoic acid by the method described by McClellan [16], purified by chromatography and characterized by NMR and mass spectrometry (MS).

*N*-vinyl-thionaphthene-indole (VTNI) was synthesized from TNI by the method already used for the *N*-vinylation of carbazole [17], purified by chromatography and characterized by NMR and MS.

Methylene chloride (Merck pro analysi) was distilled over P<sub>2</sub>O<sub>5</sub> in a nitrogen atmosphere. Tetrabutylammonium perchlorate (TBAP) (Fluka purum) was recrystallized from methanol.

Diffusion layer renewal voltammetry (DLRV), cyclic voltammetry (CV) and electrolyses were performed in 0.1 M TBAP in methylene chloride, using a multifunction AMEL Electrochemolab instrument. The reference was a saturated calomel electrode (SCE), to which all potentials are referred in this paper. The platinum counter electrode was separated from the working electrode compartment by a glass sintered disk. The working electrode was a platinum micro-electrode (1.32 mm<sup>2</sup>) for voltammetry and a platinum 1 cm<sup>2</sup> plate for electrolysis. All electrochemical experiments were carried out at room temperature (~22°C) under N<sub>2</sub> atmosphere.

The UV-vis spectral analyses were performed with a model Lambda 5 Perkin Elmer instrument.

The mass spectrometric measurements of the monomer were carried out with a Hitachi Perkin Elmer RMU 6 spectrometer: the electron impact mass spectra were obtained at 70 eV in the temperature range 50-450°C in order to check the reactivity of VTNI.

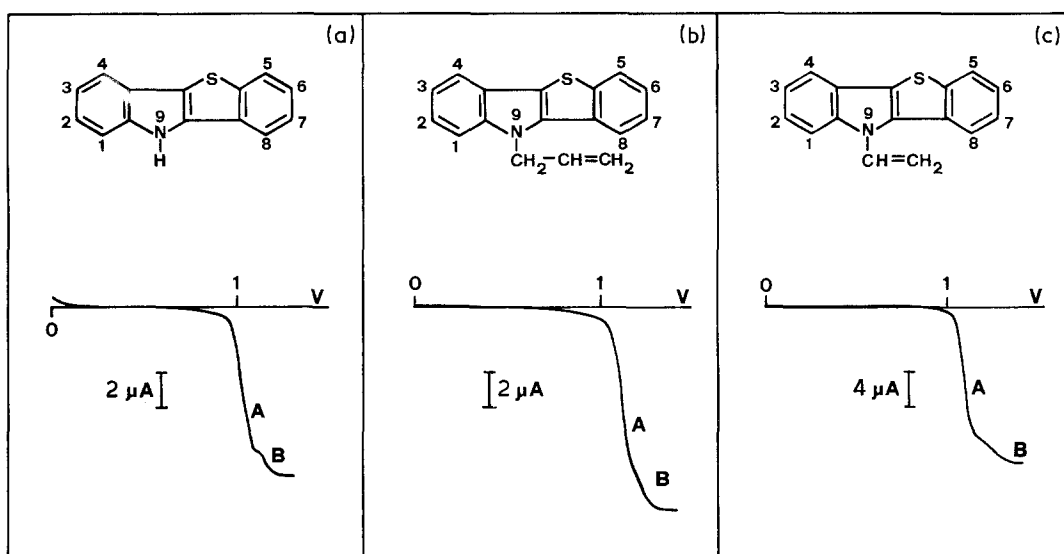


Fig. 1. Diffusion layer renewal voltammograms of (a)  $1.1 \times 10^{-3}$  M TNI, (b)  $0.97 \times 10^{-3}$  M ATNI, (c)  $1.13 \times 10^{-3}$  M VTNI in methylene chloride (0.1 M TBAP, renewal time = 2 s).

The electrolysis products were analysed with a VG ZAB 2F double focusing mass spectrometer; the mass spectra were recorded at different probe temperatures and at different times after their synthesis.

### 3. Results

The DLRV of many N-containing heterocycle compounds gives an anodic wave at about +1 V (vs SCE), which in general shows kinetic characteristics.

The literature concerning the electrochemical production of conducting polymers by oxidation of heteroaromatics containing both N and S atoms in the rings is meagre. In this respect it must be noted that thienopyrrole gives a conducting polymer [18, 19].

For the previously studied thionaphthene-indoles, the oxidation wave A, at about -1 V, is followed by a smaller one, B, at a potential not too different (Fig. 1a, b). Electrolysis on the plateau of these waves (+1.2 V) leads, for ATNI, to the oxidized dimer (with a consumption of 2 electrons per molecule) [15] and, for TNI, to the protonated dimer, the oxidized dimer and also to small amounts of oligomer, with an electron consumption ranging from 1 to more than 2, depending on experimental parameters (monomer concentration, time of electrolysis, etc.) [12, 14].

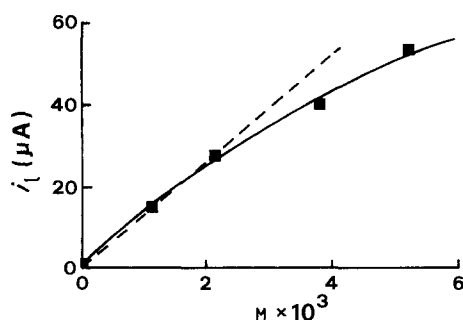


Fig. 2. Plot of limiting current of wave A ( $i_{lA}$ ) vs VTNI concentration in methylene chloride (0.1 M TBAP, renewal time = 2 s).

The DLRV of VTNI is similar to that of TNI and ATNI (Fig. 1c), showing a wave A at +1.08 V ( $c = 1.13 \times 10^{-3}$  M) and a smaller wave B (Table 1). Worthy of note is the ratio  $R = 1.86$  between the limiting currents of wave A ( $i_{lA}$ ) of VTNI and TNI, in the same experimental conditions:  $c = 1 \times 10^{-3}$  M, diffusion layer renewal time = 2 s. Moreover, for wave A of VTNI, the value of  $(RT/\alpha nF)$ , calculated from the logarithmic plot,  $E$  vs  $\log \{(i_l - i)/i_l\}$ , increases regularly with increasing concentration, while, in the cases of TNI and ATNI, this trend is not so evident ( $(RT/\alpha nF) = 61$ – $62$  mV for [TNI] =  $1$ – $2 \times 10^{-3}$  M,  $(RT/\alpha nF) = 64$  mV for [ATNI] =  $3.79 \times 10^{-3}$  M). By plotting  $i_{lA}$  vs VTNI concentration (Fig. 2), it can be seen that  $i_{lA}$  increases less than expected for a linear dependence.

As in the cases of TNI [14] and ATNI [15], the CV of VTNI (Fig. 3) shows a peak  $\alpha$ , corresponding to wave A, a peak  $\alpha'$ , corresponding to wave B, and a cathodic peak  $\beta$ , due to the reduction of the oxidation products responsible for peak  $\alpha$ . Two small peaks,  $\gamma$  and  $\delta$ , are present, at +0.25 and -0.3 V, respectively. The characteristics of  $\alpha$ ,  $\alpha'$  and  $\beta$  for VTNI are reported in Table 2. The peak  $\alpha$ , as for TNI and ATNI, shows the following kinetic features:

the peak potential  $E_{p\alpha}$  shifts anodically with increasing sweep rate,  $v$ ;

the ratio  $P = i_{p\beta}/i_{p\alpha}$ , where  $i_p$  is peak current, decreases markedly with increasing  $v$ ;

the ratio  $F = i_{p\alpha}/\sqrt{v}$  decreases with increasing  $v$ ;

$i_{p\alpha}$  does not increase linearly with the concentration, with the exception of TNI, for which a very good linearity is observed.

An aspect which markedly differentiates VTNI from its two homologues is the functional relationship between the parameter  $P$  and the concentration. In the case of ATNI [15],  $P$  decreases with increasing concentration ( $P = 0.75$  for  $c = 0.97 \times 10^{-3}$  M,  $P = 0.35$  for  $c = 3.75 \times 10^{-3}$  M). In the case of TNI [14],  $P$  is greater and decreases monotonously with the

Table 1. Characteristic parameters of diffusion layer renewal voltammetry of N-vinyl-thionaphthene-indole

	Concentration ( $M \times 10^3$ )							
	1.13		2.14		3.79		5.20	
	Wave A	Wave B	Wave A	Wave B	Wave A	Wave B	Wave A	Wave B
$E_{1/2}$ (V)	1.08	1.22	1.09	1.25	1.06	1.26	1.06	1.25
$i_1$ ( $\mu A$ )	15.6	1.6	27.4	3.4	40.0	6.4	55.6	8.8
$i_B/i_A$	0.104		0.126		0.160		0.160	
$E$ vs $\log \{(i_1 - i)/i\}$	48-52		66		78		83	
slope (mV)	1.13-1.23		0.89		0.76		0.71	
$\alpha n$	1.13-1.23		0.89		0.76		0.71	

concentration, as shown in Fig. 4. However, for VTNI  $P$  increases with increasing concentration; only at very low sweep rates ( $v = 20$  and  $50 \text{ mV s}^{-1}$ ) is a small decrease of  $P$  observed for high concentrations.

The ratio  $i_{px'}/i_{px}$ , although not easily calculable, also shows an increasing trend with increasing concentration.

Remarkable differences between VTNI and its two homologues emerge from the results of electrolysis experiments at  $+1.2 \text{ V}$ , which, in the case of VTNI, depend strongly on concentration. At low concentrations ( $c \leq 1 \times 10^{-3} \text{ M}$ ) the oxidized dimer is obtained, with a consumption of 2.3-2.5 electrons per molecule; the spectrum of the blue-violet solution of the product in the reaction medium is very similar to those of TNI and ATNI in the same conditions (Fig. 5). The final DLRV shows a cathodic wave C ( $E_{1/2} = +0.25 \text{ V}$ ) and a second wave D ( $E_{1/2} = -0.17 \text{ V}$ ) (Fig. 5a, inset 1), in equilibrium with C: in effect, by electrolysis at  $0 \text{ V}$ , wave D decreases. For wave C, the value of  $RT/\alpha nF$ , calculated from the logarithmic plot,  $E$  vs

$\log \{(i_1 - i)/i\}$ , increases with time (from 49 to 68 mV). The ratio  $G = i_{1C}/i_{1D}$  is not constant and depends strongly on the experimental conditions of electrolysis.

By electrolysis on cathodic wave C, a decrease of the spectral visible bands is observed (Fig. 6). The same figure shows the behaviour with time of waves C and D and of the spectral bands of the dimer dication, recorded after alternate electrolysis and stand-by periods. In the final voltammetry an anodic current is observed. This current, however, in contrast to ATNI, does not give a defined wave which anticipates that of the unelectrolysed monomer, but occurs at more positive potentials.

By electrolysis more concentrated VTNI solutions ( $c = 5 \times 10^{-3} \text{ M}$ ) at  $+1.2 \text{ V}$ , a different behaviour is observed: black oxidized polymer is formed and a low constant current is attained when the electron consumption is about 2.5 electrons per molecule (this value is not too different from that measured when dimer is produced at low VTNI concentrations).

Table 2. Characteristic parameters of cyclic voltammetry of N-vinyl-thionaphthene-indole

Sweep rate, $v$ ( $\text{mV s}^{-1}$ )		Concentration ( $M \times 10^3$ )											
		1.13			2.14			3.79			5.20		
		$\alpha$	$\alpha'$	$\beta$	$\alpha$	$\alpha'$	$\beta$	$\alpha$	$\alpha'$	$\beta$	$\alpha$	$\alpha'$	$\beta$
20	$E_p$ (V)	1.10	1.20	0.96	1.10	1.22	0.97	1.10	1.24	0.96	1.14	1.29	0.96
	$i_p$ ( $\mu A$ )	6.3		0.1	17.4		0.6	27.6		1.6	35.2		1.6
	$P = i_{p\beta}/i_{px}$		0.016			0.037			0.058			0.045	
	$F = i_{px}/\sqrt{v^*}$		1.409			3.890			6.172			7.870	
50	$E_p$ (V)	1.15		0.99	1.13	1.24	0.99	1.13	1.26	0.98	1.18	1.32	0.98
	$i_p$ ( $\mu A$ )	9.8		0.7	23.8		1.8	37.2		4.0	47.2		4.8
	$P = i_{p\beta}/i_{px}$		0.070			0.076			0.108			0.102	
	$F = i_{px}/\sqrt{v^*}$		1.386			3.366			5.261			6.675	
100	$E_p$ (V)	1.17		0.99	1.14	1.24	0.98	1.13	1.24	0.97	1.22	1.33	0.98
	$i_p$ ( $\mu A$ )	13.0		1.0	29.6		4.4	47.2		8.0	60.0		10.4
	$P = i_{p\beta}/i_{px}$		0.077			0.149			0.169			0.173	
	$F = i_{px}/\sqrt{v^*}$		1.300			2.960			4.720			6.000	
200	$E_p$ (V)	1.21		1.00	1.19		0.98	1.19	1.30	0.98	1.27	1.37	0.96
	$i_p$ ( $\mu A$ )	17.8		1.6	39.2		6.8	63.6		15.2	77.6		20.8
	$P = i_{p\beta}/i_{px}$		0.090			0.173			0.239			0.268	
	$F = i_{px}/\sqrt{v^*}$		1.259			2.772			4.497			5.487	

\*  $F$  dimensions:  $\mu A s^{1/2} \text{ mV}^{-1/2}$ .

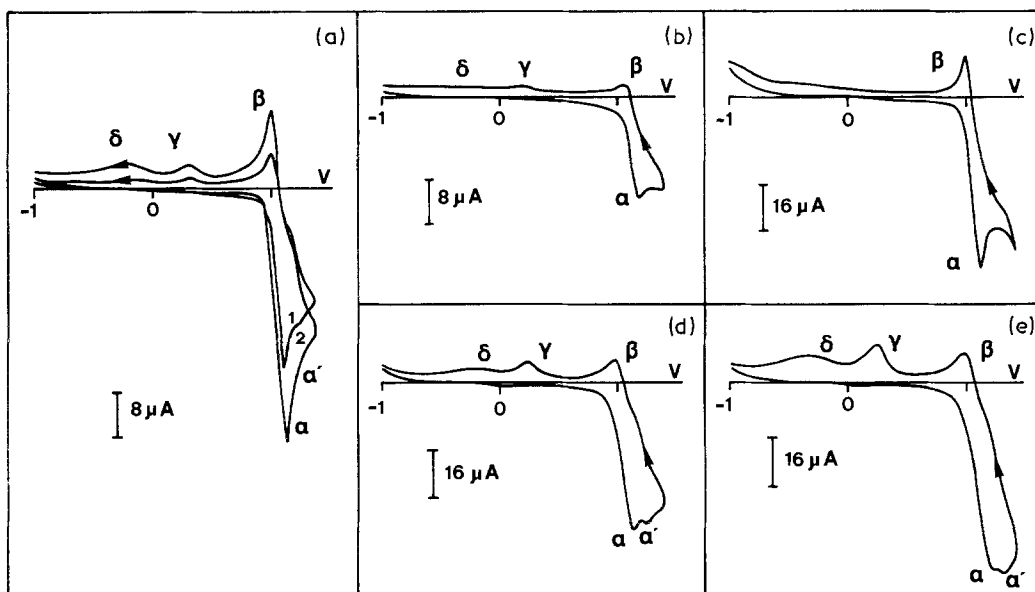


Fig. 3. Cyclic voltammeteries in methylene chloride (0.1 M TBAP) of (a)  $1.13 \times 10^{-3}$  M TNI [sweep rates: (1)  $50 \text{ mV s}^{-1}$ , (2)  $100 \text{ mV s}^{-1}$ ], (b)  $0.97 \times 10^{-3}$  M ATNI ( $100 \text{ mV s}^{-1}$ ), (c)  $1.00 \times 10^{-3}$  M VTNI ( $100 \text{ mV s}^{-1}$ ), (d)  $3.79 \times 10^{-3}$  M VTNI ( $100 \text{ mV s}^{-1}$ ), (e)  $5.20 \times 10^{-3}$  M VTNI ( $100 \text{ mV s}^{-1}$ ).

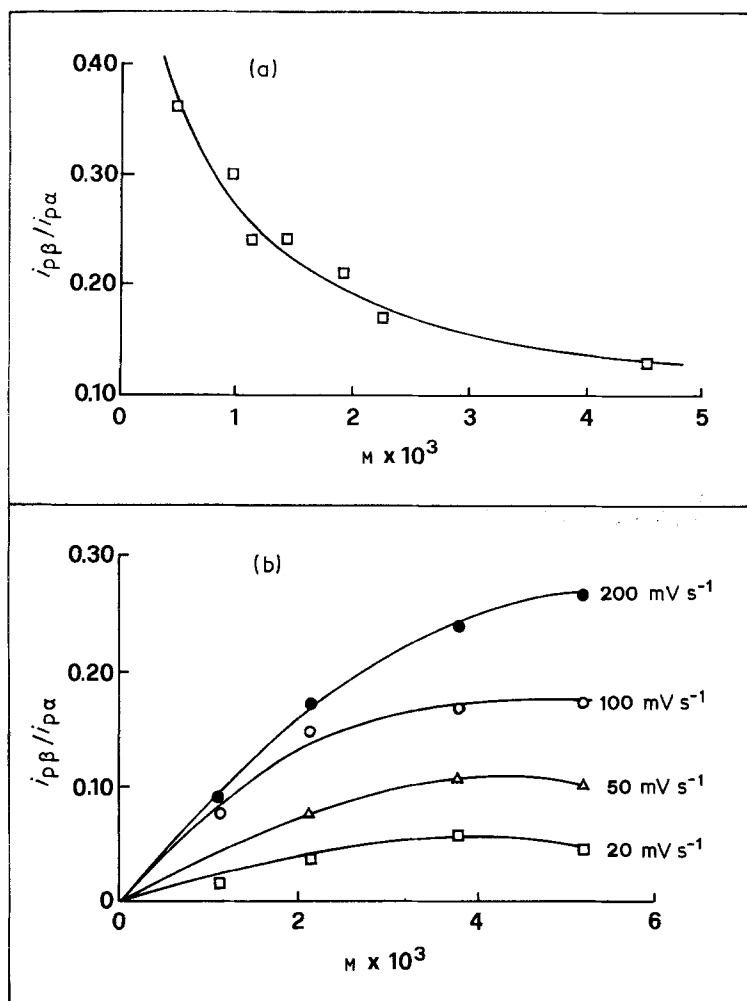


Fig. 4. Plot of peak current ratio  $i_{p\beta}/i_{p\alpha}$  vs concentration in methylene chloride (0.1 M TBAP) of (a) TNI (sweep rate:  $100 \text{ mV s}^{-1}$ ), (b) VTNI (several sweep rates).

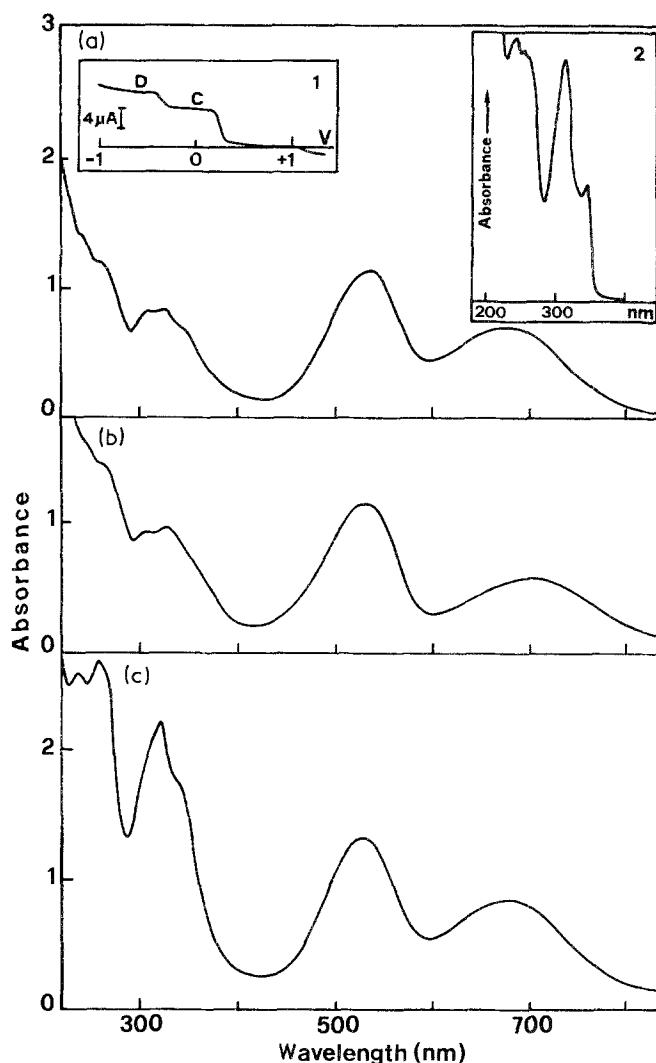


Fig. 5. Absorption spectra recorded after the flow of (a) 8.09 C in 40 ml of  $1.00 \times 10^{-3}$  M VTNI, (b) 10.94 C in 50 ml of  $1.08 \times 10^{-3}$  M ATNI, (c) 13.92 C in 40 ml of  $1.92 \times 10^{-3}$  M TNI, in methylene chloride (0.1 M TBAP, optical path = 0.1 cm). Insets: (1) diffusion layer renewal voltammetry corresponding to absorption spectrum of (a); (2) UV spectrum of unelectrolysed VTNI in methylene chloride [optical path = 0.1 cm, extinction coefficients:  $\epsilon$  (242 nm) = 22 000,  $\epsilon$  (312 nm) = 20 600].

Depending on the experimental conditions, the black solid can deposit as a film on the electrode or as a powder on the cell bottom.

By electrolysis of  $5 \times 10^{-2}$  M VTNI solutions at +1.2 V, a black oxidized insoluble polymer is obtained

and, more rapidly than at lower concentrations, a low constant current is achieved with a consumption of 0.9–1.3 electrons per molecule. The black solid is obtained with a 76% yield (52 mg from 50 mg VTNI), by assuming the formula calculated from elemental analysis and mass spectrometry results.

The mass spectrum of this product shows peaks of ions having high mass unit, which are congruent with a polymeric material. The spectrum, obtained at a source temperature of 160°C from the electrolysis products of a high concentrated monomer solution, is shown in Fig. 7. Numerous peaks relative to double charged ions, not well defined in the figure, are also present: the  $m/z$  values = 110.5, 111.5, 112.5, 128.5, 129.5, 164.5, 178.5, 204.5, 221.5, 222.5, 239.5, 261.5, 267.5, 291.5, 309.5, 356.5, corresponding respectively to  $m = 221, 223, 225, 257, 259, 329, 357, 523, 583, 619, 713$  amu are of particular interest.

The mass spectra of VTNI, recorded in the temperature range 50–450°C, do not show any peaks at  $m/z > 249$  and this excludes the possibility of dimerization or oligomerization of the monomer in the ion source.

The elemental analysis of the electrolysis product

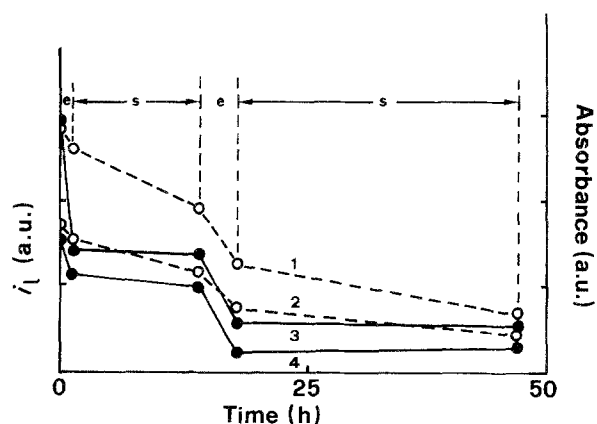


Fig. 6. Values of (1) absorbance at 530 nm, (2) absorbance at 680 nm, (3) limiting current of waves C + D, (4) limiting current of wave C, recorded after alternate electrolysis at 0 V (e) and stand-by (s) periods, of  $9.04 \times 10^{-4}$  M VTNI in methylene chloride (0.1 M TBAP) electrolysed at +1.2 V.

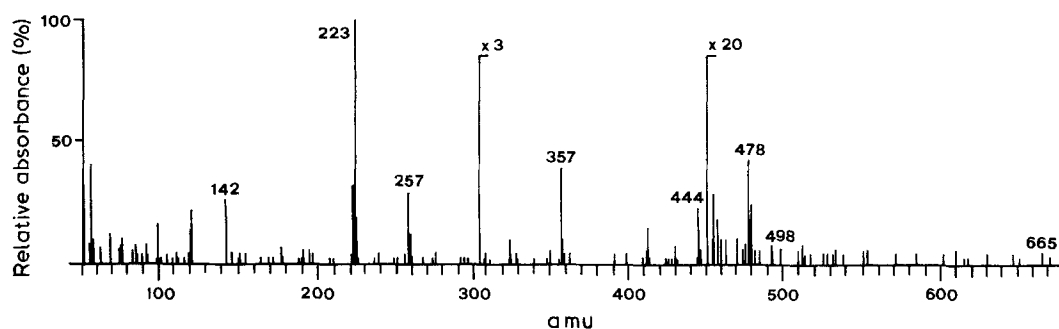
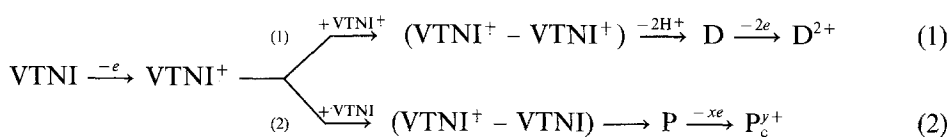


Fig. 7. Electron impact mass spectrum (70 eV, 200  $\mu$ A) of the solid product obtained by electrolysis at +1.2 V of  $5 \times 10^{-2}$  M VTNI in methylene chloride (0.1 M TBAP) (source temperature = 160°C).

gives the following per cent composition: C 58.68, H 3.56, N 4.43, O 15.77, S 9.99, Cl 7.56.

#### 4. Discussion

The electrochemical behaviour of VTNI, by oxidation at +1.2 V, which in some aspects differs from those of TNI and ATNI, agrees with the overall kinetics of Scheme 1:

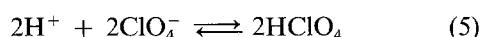
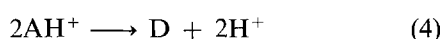


Scheme 1.

At relatively low concentrations of VTNI, the coupling should involve two cations, as in the cases of TNI and ATNI, with production of dimer D, then oxidized to  $\text{D}^{2+}$  with an overall consumption of about 2 electrons per monomer unit.

It must be noted that the limiting current ratio  $R$  for wave A of VTNI over TNI, at low concentrations, is 1.8–1.9. Also, under the same experimental conditions, the height of wave A increases in the order: TNI < ATNI < VTNI. Because it is reasonable to consider wave A of TNI as monoelectronic ( $RT/\alpha nF$ , from the logarithmic plot, is 60 mV [14]), wave A of VTNI is then bielecronic and correlated to a fast formation of  $\text{D}^{2+}$ .

In this last case, besides the intervention of a faster coupling of the radical cations, the production of an oxidized dimeric species is made easier by a shift to the left of equilibrium 6 between the dimer and  $\text{HClO}_4$  produced by electrolysis:



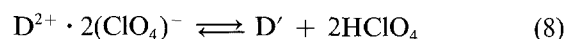
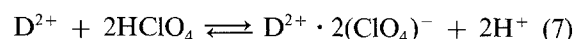
(AH is the monomer; D is the dimer;  $\text{HClO}_4$  can be an undissociated molecule or an ion pair, depending on the ionization of perchloric acid in methylene chloride, about which no report has been found in the literature.)

The higher reactivity of VTNI in comparison

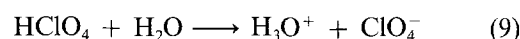
with TNI for coupling and subsequent reactions of Scheme 1, leading to dioxidized dimer  $\text{D}^{2+}$ , is also supported by the cyclic voltammetry ratio  $P$  (Fig. 3), which is greater for TNI at almost all the experimental concentrations.

After electrolysis two cathodic waves, C and D, appear in the voltammogram of low concentration VTNI solutions. Wave C was attributed, as well as for TNI [14] and ATNI [15], to reduction of an adduct

involving the dimer dication and  $\text{HClO}_4$ . That waves C and D, and the corresponding peaks  $\gamma$  and  $\delta$ , are connected to several equilibria between dimer dication and  $\text{HClO}_4$  is probable if, besides the effects on these waves of the subsequent electrolysis at the potential of wave C, those on the visible spectral bands are also taken into consideration (Fig. 6). These equilibria are schematically represented by the equations below:



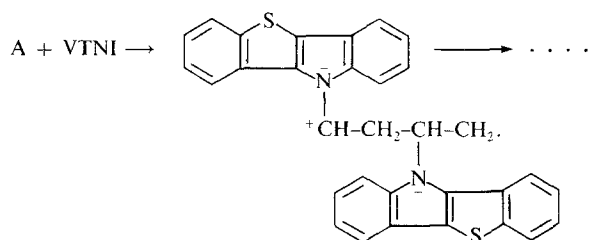
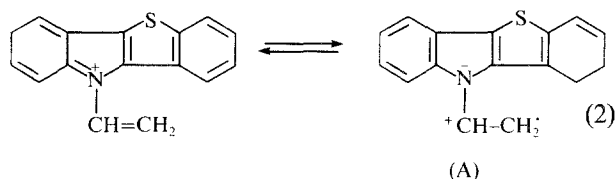
and, eventually, owing to possible traces of water in the sample



The two waves are due to the reduction of  $\text{HClO}_4$  involved in these equations or also to the direct reduction of the dimer dication. The fact that, for wave C, the logarithmic plot slope ( $RT/\alpha nF$ ) changes with time, while the wave height does not, could be due to equilibrium 8 moving right. The fact that, by electrolysis on this wave, an anodic wave is obtained only at more positive potential than that of the monomer could mean that the neutral dimer is not produced, but different species, maybe oligomers, are formed and that the electrode kinetics connected to the reduction of the dioxidized dimer are complex.

At higher VTNI concentrations, process 2 of Scheme 1, which is a real chain polymerization occur-

ring with low consumption of electrons per molecule, is more important:



Obviously, the polymer produced in this way, or the monomer, can be oxidized, with coupling involving the benzene rings, release of hydrogen ions and further oxidation of the aromatic part leading to an oxidized cross-linked polymer  $P_c^+$ .

The slope of the DLRV logarithmic plot of wave A indicates a decrease of the factor  $\alpha n$  with increasing VTNI concentration (Table 1), owing to either a decrease of the amount of electrons per molecule or/and to a lower reversibility of the electron transfer (parameter  $\alpha$ ). The decrease in  $\alpha$  may be due to the formation of a thin deposit of adsorbed molecules on the electrode (due to a faster formation of condensed species with respect to TNI and ATNI). Moreover, the heights of wave A and peak  $\alpha$  do not change linearly with VTNI concentration.

That the oxidation mechanism of VTNI is different from that of TNI and ATNI is also supported by the ratio  $P$ , which generally increases with increasing VTNI concentration. This behaviour may be due to such a closeness between the reduction potentials of  $(VTNI)_x^+$  and  $(VTNI)^+$  that the two cathodic peaks cannot be discriminated. A kinetic treatment of this process appears to be complex; anyway, it is beyond the scope of the present work.

In the case of TNI, the electrode process associated to wave B and to the corresponding peak  $\alpha'$ , the importance of which increases with increasing monomer concentration, was suggested to be the oxidation of the dimer of the radical cation, subsequent to the first deprotonation, and/or the oxidation of the protonated dimer or of the protonated monomer. These are minor processes in the case of VTNI, probably owing to a minor incidence of the ring coupling with respect to the chain coupling to a smaller stability constant of the protonated monomer.

The mechanism of Scheme 1 is strongly supported by the results of electrolytic experiments. Electrolysis at +1.2 V of highly concentrated solutions of VTNI

leads to a polymer with an electron consumption which decreases with increasing monomer concentration. As stated earlier, ATNI, which differs from VTNI just in the allyl double bond, does not give polymer but only oxidized dimer, as do low concentrated VTNI solutions. This is probably due to the asymmetry of the molecule, which does not allow all the sites of the aromatic rings to be active in the coupling reaction of radical cations but is overcome, in the case of highly concentrated VTNI, by the reactivity of the side chain, favoured by the conjugation between the aromatic moiety and the vinyl double bond.

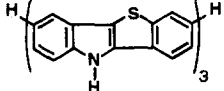
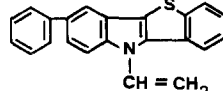
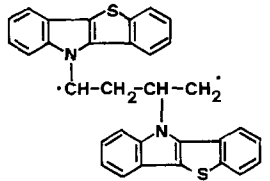
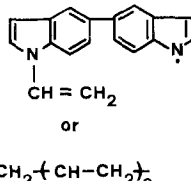
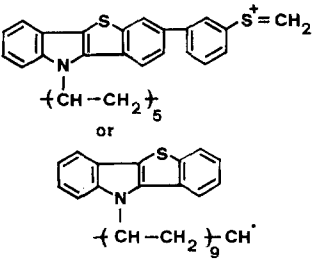
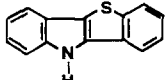
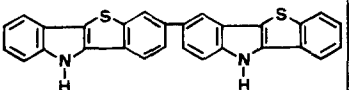
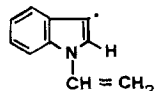
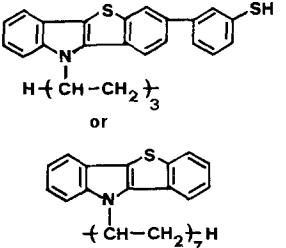
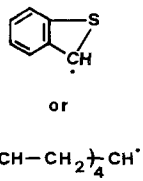
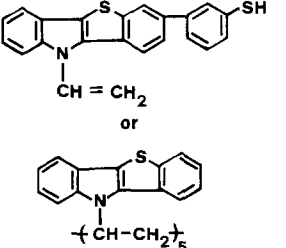
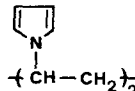
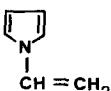

Moreover, the mass spectra of the electrolysis products of VTNI show peaks corresponding to a mass unit higher than the trimer mass and confirm the presence of polymeric chains. The mass spectrum of Fig. 7, obtained at 160°C, is characterized by the presence of peaks corresponding to  $m/z = 223, 444, 665$ , which could originate by polymerization due to the active sites of the aromatic rings; it is evident that the drastic conditions of electron impact favour the loss of vinyl groups. Table 3 shows the possible structure of some of the more significant ionic species and, on this basis, it is reasonable to suggest the presence of polymer grown by coupling involving both the vinyl groups and/or the benzene rings. Some deprotonation of monomer and dimer is evident and this could be due to cross-linked material. The numerous double charged ions agree with stable structures with mass up to 713 amu.

The same material, analysed some months later, gives a good mass spectrum in the same mass spectrometric conditions only at  $T \geq 200^\circ\text{C}$ . This result can be ascribed to a more cross-linked polymer and the more drastic temperature brings out different ionic species: in particular, the absence of peaks relative to polymerization involving benzene rings is noted.

The formula calculated from the elemental analysis of freshly prepared product,  $C_{15.7}H_{11.3}S_1N_{1.01} \cdot 0.682(Cl_1O_{4.57})$ , suggests that the vinyl group remains attached to the monomer unit during the polymerization and is in accord with a reaction mainly involving the side chains, if the high hydrogen content is taken into consideration. Anyway, in this formula the oxygen and hydrogen amounts are greater than the theoretical values. This could be due to traces of water present in the sample, as found for other similar materials. Considering this possibility, the repeat unit becomes:  $C_{15.7}H_{10.5}S_1N_{1.01} \cdot 0.682(ClO_4) + 1.3H_2O$ . In this case, the small difference of the hydrogen content with respect to the theoretical formula ( $C_{16}H_{11}SN$ ) could be attributed to parallel coupling involving aromatic rings and leading to cross-linked structures.

It is also worth noting the absence of detectable amounts of supporting electrolyte in the electrolysis product, unlike the finding in the case of poly-TNI and poly-ATNI. This is reasonably attributable to the fact that, while the polymerization of TNI and ATNI is performed at relatively high potentials (about +3 V), the polymerization of VTNI is possible at +1.2 V.

Table 3. Results of mass spectrometry measurements on poly-VTNI

m/z	empirical formula	structure formula	m/z	empirical formula	structure formula
665	$C_{42}H_{23}N_3S_3$		325	$C_{22}H_{15}NS$	
498	$C_{32}H_{22}N_2S_2$		257	$C_{18}H_{13}N_2$ or $C_{19}H_{29}$	
478	$C_{31}H_{28}NS_2$ or $C_{33}H_{36}NS$		223	$C_{14}H_9NS$	
444	$C_{28}H_{16}N_2S_2$		142	$C_{10}H_8N$	
412	$C_{26}H_{22}NS_2$ or $C_{28}H_{30}NS$		121	$C_7H_5S$ or $C_9H_{13}$	
357	$C_{22}H_{15}NS_2$ or $C_{24}H_{23}NS$		120	$C_8H_{10}N$	
			93	$C_6H_7N$	
			78	$C_6H_6$	

## 5. Conclusions

The vinyl side group allows VTNI to polymerize to oxidized polymer by electrolysis at +1.2V while, in the case of the allyl derivative (ATNI), only an oxidized dimer is obtained. Moreover, poly-VTNI has a molecular weight greater than that of poly-TNI and poly-ATNI, due to the formation of a macromolecule with intermonomer bonds involving both the aliphatic chains and the aromatic rings. The experimental results agree with literature reports concerning a similar

molecule, *N*-vinyl-carbazole, where the formation of a cross-linked polymer by reaction both in the aliphatic and in the aromatic moiety is suggested.

Studies of the electroconductivity and photoconductivity properties of poly-VTNI will be reported in a further paper.

## Acknowledgements

The technical assistance of Mr B. Facchin in the mass spectrometry measurement is acknowledged. The



authors thank also Mr G. Gubellini for drawing the figures.

This work has been supported by Progetto Strategico "Nuovi Materiali" of National Research Council of Italy (C.N.R.).

## References

- [1] J. F. Ambrose and R. F. Nelson, *J. Electrochem. Soc.* **115** (1968) 1159.
- [2] A. Desbène-Monvernay, P. C. Lacaze and J. E. Dubois, *J. Electroanal. Chem.* **129** (1981) 229.
- [3] D. H. Davies, D. C. Phillips and H. D. B. Smith, *J. Org. Chem.* **38** (1973) 2562.
- [4] B. R. Hsieh, M. H. Litt and K. Abbey, *Macromolecules* **19** (1986) 521.
- [5] A. Desbène-Monvernay, J. E. Dubois and P. C. Lacaze, *J. Electroanal. Chem.* **189** (1985) 51.
- [6] Y. Shirota, N. Noma, H. Kanega and H. Mikawa, *J. Chem. Soc., Chem Commun.* (1984) 470.
- [7] M. G. Cross, D. Walton, N. J. Morse, R. J. Mortimer, D. R. Rosseinsky and D. E. Simmonds, *J. Electroanal. Chem.* **189** (1985) 389.
- [8] A. F. Diaz, J. Crowley, J. A. Logan and W. J. Lee, *J. Electroanal. Chem.* **129** (1981) 115.
- [9] R. J. Waltman, A. F. Diaz and J. Bargon, *J. Phys. Chem.* **88** (1984) 4343.
- [10] G. Casalbore-Miceli, G. Beggato, P. G. Di Marco, S. S. Emmi, G. Giro and B. Righetti, *Synth. Met.* **15** (1986) 1.
- [11] G. Casalbore-Miceli, G. Beggato, S. Daolio, P. G. Di Marco, S. S. Emmi and G. Giro, *J. Appl. Electrochem.* **17** (1987) 1111.
- [12] G. Beggato, G. Casalbore-Miceli, S. S. Emmi, P. G. Di Marco, G. Giro and G. Poggi, *Bull. Soc. Chim.* (1988) 301.
- [13] G. Giro, G. Beggato, G. Casalbore-Miceli, P. G. Di Marco and S. S. Emmi, *Mol. Cryst. Liq. Cryst.* **156** (1988) 311.
- [14] G. Casalbore-Miceli, G. Beggato, S. Daolio, S. S. Emmi, A. Geri and B. Righetti, *J. Chem. Soc., Perkin Trans. II* (1988) 1231.
- [15] G. Casalbore-Miceli, G. Beggato, S. Daolio, P. G. Di Marco, S. S. Emmi and G. Giro, *Ann. Chim. Rome* **77** (1987) 609.
- [16] E. W. McClellan, *J. Chem. Soc.* (1929) 1588.
- [17] G. R. Clemo and W. H. Perkin, *J. Chem. Soc. Trans.* **125** (1924) 1804.
- [18] R. Lazzaroni, J. Riga, J. J. Verbist and M. Renson, *J. Chem. Soc., Chem. Commun.* (1985) 999.
- [19] R. Lazzaroni, A. De Prijck, J. Riga, J. Verbist, C. Bonhomme, F. Brose, L. Christiaens and M. Renson, *Synth. Met.* **18** (1987) 123.